ISSN 0967-0912, Steel in Translation, 2019, Vol. 49, No. 12, pp. 848–853. © Allerton Press, Inc., 2019.
Russian Text © The Author(s), 2019, published in Izvestiya Vysshikh Uchebnykh Zavedenii, Chernaya Metallurgiya, 2019, No. 12, pp. 964–971.

High-Power Current-Pulse Generator Based on a Reverse Thyristor Converter

V. A. Kuznetsov[a], *, G. D. Polkovnikov[a], **, V. E. Gromov[a], *, E. S. Kuznetsova[a], ****, and O. A. Peregudov[b], *******

[a]*Siberian State Industrial University, Novokuznetsk, 654007 Russia*
[b]*Omsk State Technical University, Omsk, 644050 Russia*
**e-mail: vladimir.kuznezoff@yandex.ru*
***e-mail: george42rus@gmail.com*
****e-mail: gromov@physics.sibsiu.ru*
*****e-mail: kuzlena00@yandex.ru*
******e-mail: olegomgtu@mail.ru*

Received April 16, 2019; revised May 8, 2019; accepted May 14, 2019

Abstract—In metal processing by powerful current pulses, there is a need for adjustment of both the pulse repetition rate and amplitude. This paper describes a powerful current-pulse generator with a controlled thyristor converter, which is used as a power source for a charging device for regulating the voltage (pulse amplitude) of a capacitor charge. The disadvantages of the generators associated with the current spike in the capacitor charge modes that reduces the supply network quality are discussed. The application of a reverse thyristor converter (RTC) as a power supply is considered to reduce the transient time at a voltage decrease on the capacitors. The generator's structural diagram that consists of a reversible thyristor converter with separate control, a power unit, a capacitor recharge device, an automatic control system (ACS) for the charger parameters, and a capacitor charging control system is presented. The regulator parameters of the ACS are calculated. To obtain optimal transients, a standard methodology for regulator tuning according to a modular optimum is employed. In order to reduce overadjustment at the disturbance time reaching 100% and higher, the so-called logical device is introduced into the ACS. The latter blocks the control pulses on the converter thyristors and simultaneously reduces the signal at the output of the current regulator to zero. A simulation model of a powerful current pulse generator is synthesized in the MatLab-Simulink environment. The model is analyzed, and plots explaining the device's operation principle and transients in various operating modes are shown. The use of a generator will allow high-performance adjustments of the current pulse amplitude and obtain sufficiently high-quality capacitor charge (discharge) transients, which will have a beneficial effect on the power supply network. The application of higher quality converters will significantly increase the current pulse repetition rate.

Keywords: powerful current pulse generator, generator charger, system for automatically adjusting generator parameters, control circuits for capacitor voltage and charge current

DOI: 10.3103/S0967091219120064

INTRODUCTION

Discovered over 50 years ago, the electroplastic effect is widely used to intensify the processing of hardly deformed steels and alloys in the metallurgical, automotive, and machine-building industries [1–6]. An analysis of the studies of Chinese and American researchers in recent years shows that the addition of powerful short current pulses to the deformation zone during pressure treatment (rolling, drawing, pressing, etc.) significantly changes the material's structural phase states and provides a reduction in the energy-power parameters of the processes [7–25]. For electrostimulated material processing, sources of powerful short current pulses are needed.

With the advent of high-speed high-power thyristors, powerful unipolar-current pulse generators that discharged pre-charged capacitors to a low-impedance load through a thyristor switch were developed. The most important generator component is the charger generally containing non-controlled or controlled rectifier [26].

Figure 1 shows a powerful current pulse generator with the following parameters: supply voltage is 3 × 380 V; the duration and amplitude of unipolar sine wave pulses are 150 μs and 15 kA, respectively; pulse repetition rate is 0–200 Hz; and equivalent capacitance is 1000 μF.

Electrically stimulated metal processing is characterized by high requirements for the transient quality and the high-speed performance of the current pulse generator. This leads to the need to develop ACSs for power parameters. Manual or poor-quality regulation usually leads to equipment breakdown and increased defects [27].

The generator can operate in two modes: repetition rate adjustment or current pulse amplitude. For electrically stimulated drawing, the first operation mode when the repetition rate of current pulses changes over a wide (0–500 Hz) range is usually used. Regulation mode operation of the pulse amplitude is required, i.e., in cases of the processed wire's insignificant diameter. In this case, a large amplitude pulse can lead to a break in the workpiece due to a dynamic shock or overheating. The pulse amplitude control is possible in the heat drawing modes of the workpiece, as well as rolling and stamping.

This work is aimed at developing and creating a powerful current pulse generator with a controlled converter as a charger power supply to control the pulse parameters.

RESULTS AND DISCUSSION

Here, we study the generator's operating mode with the amplitude adjustment of the current pulses by changing the power capacitor voltage. The voltage adjustment on the capacitors can be performed, i.e., using a non-reversible thyristor converter as an adjustable power supply of a charging device (charger) [28]. The disadvantage of this method is the absence of the charger current's negative component (discharge current), which leads to an uncontrolled long capacitor discharge and a significant generator speed decrease if the pulse amplitude is reduced. To eliminate this drawback, an RTC is applied in a powerful pulse generator, the structural diagram of which is shown in Fig. 2.

The generator contains a charger with an RTC consisting of oppositely connected thyristor bridges *SV*1 and *SV*2, which is connected to the capacitors *CB* through series-connected equivalent active resistance *R*1 and inductance *L*1, a capacitor discharge block with the load (capacitors *CB*, thyristor switch *VS*3, and load *R*l), recharge unit *YP* (transformer *M*, diode *VD*1, resistor *R*3, and amplifier *G*3 with limiting unit *S*3), with actions described in [29], as well as an auto ACS of generator parameters (voltage setting unit *BZU*, regulators *RNZ* and *RU*, and sensors of the main parameters *DTZ* and *DU*).

To analyze the generator's dynamic operating modes, a simulation model that contains the above listed blocks was created in the MatLab-Simulink environment (Fig. 3). The names of the block elements in the structural diagram and in the model are identical.

Fig. 1. Appearance of a powerful current pulse generator [26]: (*1*) a system for generating control pulses, (*2*) thyristor converter blocks, (*3*) capacitor banks, (*4*) fan, and (*5*) drawing mill.

The ACS of the generator charger parameters is designed as a subordinate control system and contains two control loops: an internal one is for the control of the capacitor charge current (hereinafter, referred to as a current loop) consisting of a proportional-integral (PI) current regulator *RTZ*, an RTC, an adjustment object, and feedback containing low-inertia current sensor *DTZ* while an external loop is for the voltage control on capacitors (hereinafter, referred to as voltage loop) consisting of a proportional (P)-voltage regulator *RU*, an optimized current circuit, an adjustment object (capacitors *CB*), and also a voltage feedback sensor *DU*. The above loops are tuned to the modular optimum.

The transfer function of the W_{TC} thyristor converter is equal to 30:

$$W_{TC} = \frac{K_{TC}}{T_{\mu TC} + 1}, \tag{1}$$

where $K_{TC} = 60$ and $T_{\mu TC} = 5$ ms are the gain coefficient and the small (uncompensated) time constant of the thyristor converter, respectfully.

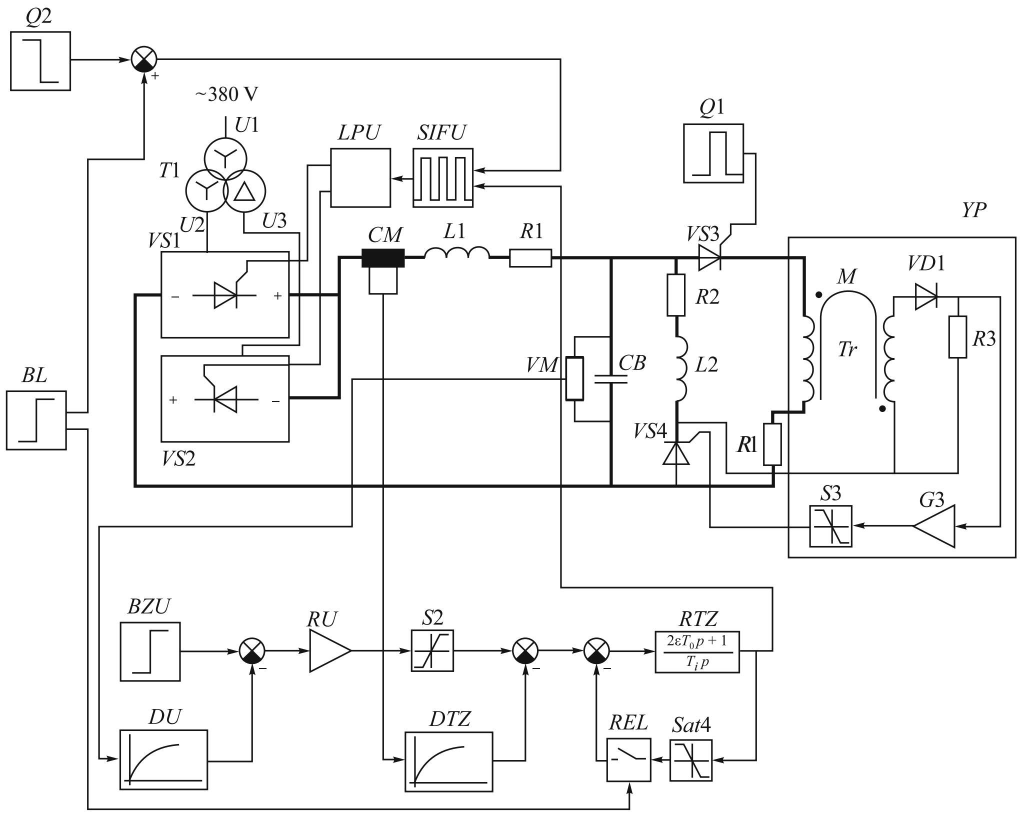

Fig. 2. ACS structural diagram of the generator of high-power current pulses.

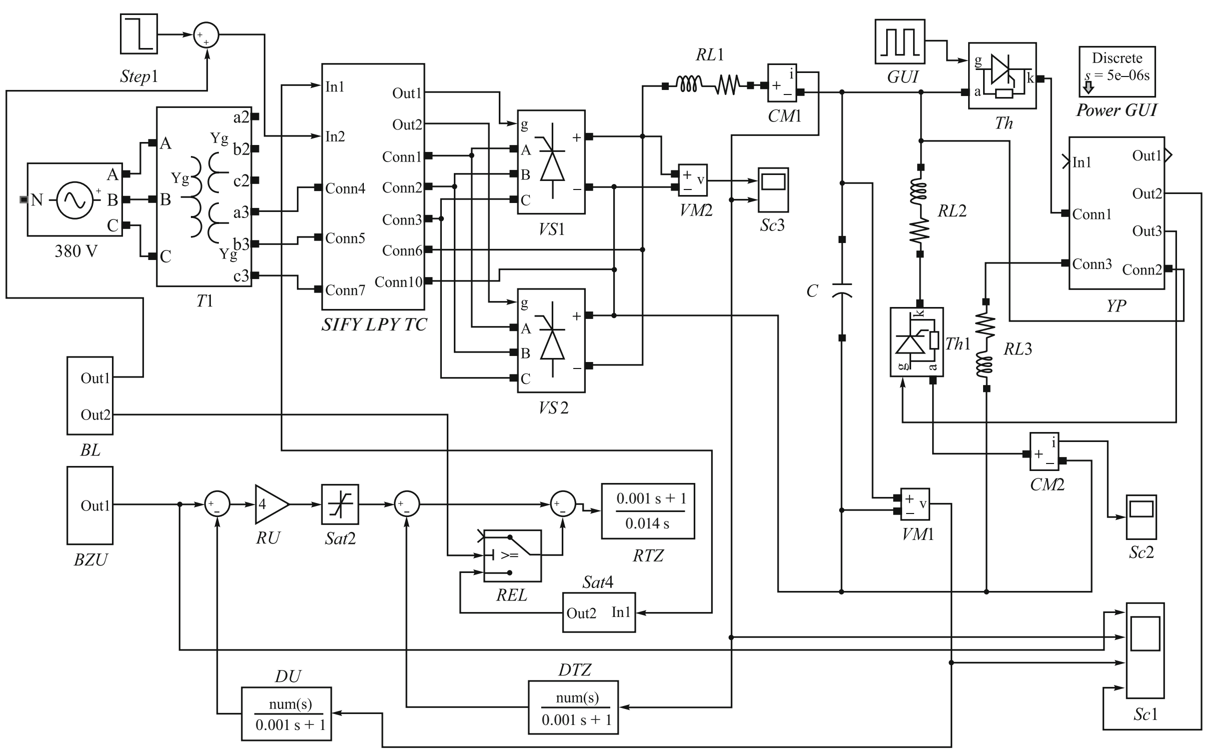

Fig. 3. Model of a generator with a reversing converter.

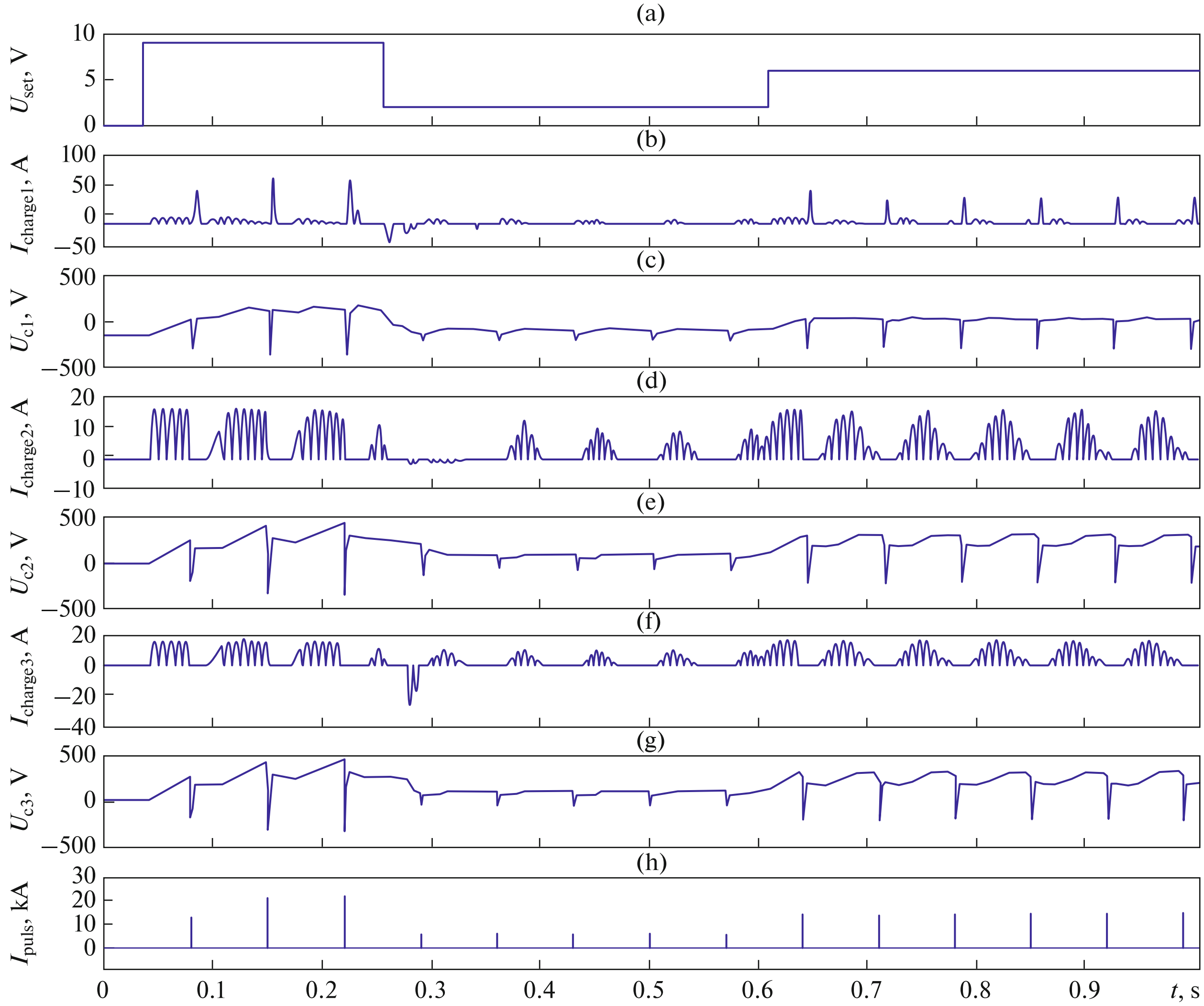

Fig. 4. Charger transient plots of the current pulse generator: (a) signal for setting the capacitor voltage (U_{set}), (b) charge (discharge) current ($I_{charge1}$) of the charger with a reversing converter without the *BL*, (c) capacitor voltage (U_{c1}) using a charger with a reversing converter without a *BL* unit, (d) charge (discharge) current ($I_{charge2}$) of a charger with a non-reversing converter, (e) capacitor voltage (U_{c2}) using a charger with a non-reversing converter, (f) charge (discharge) current ($I_{charge3}$) of capacitors with a reversing converter, (g) capacitor voltage (U_{c3}) using a charger with a reversing converter, and (h) current pulses (I_{puls}) of the generator.

The transfer function W_{OC} of the adjusting object has the charge current in the following form:

$$W_{OC} = \frac{1/C}{T_o^2 p^2 + 2\xi T_o p + 1}, \quad (2)$$

where C is the capacitance of the capacitor bank, F; T_o is the time constant of the oscillatory current loop, s; ξ is the attenuation coefficient of the oscillatory current loop; and p is the Laplace operator.

The transfer function W_{OV} of the voltage adjustment object on the capacitors is equal to:

$$W_{OV} = \frac{1}{C}. \quad (3)$$

The results of tuning the ACS are shown in Fig. 3.

If $T_o^2 \geqslant 2\xi T_o$, then the entity $T_o^2 p^2$ in formula (2) can be neglected. In this case, the transfer function of the current adjustment object is simplified and has the following form:

$$W_{OC} = \frac{1/C}{2\xi T_o p + 1}. \quad (4)$$

It is known that a PI controller is used when tuning to a modular optimum, and its transfer function has the following form:

$$W_{rt} = \frac{2\xi T_o p + 1}{T_i p}, \quad (5)$$

where the time constant is determined by the formula

$$T_i = 2T_{\mu TC}(CK_{TC}K_{CS}), \tag{6}$$

here, K_{CS} is the current sensor gain coefficient.

Resistance $R1$ consists of a series-connected equivalent resistance of the charging circuit (active resistance of the transformer windings, converter busbars and thyristors, etc.), as well as an additional resistor, and is selected from the conditions for minimizing power losses on the resistance. For the specified generator, the resistance should be 0.5–1.0 Ohms. The inductance $L1$ is selected so that the condition $T_o^2 \geqslant 2\xi T_o$ is satisfied.

The voltage regulator is designed as a proportional regulator with a gain coefficient of $k_{pc} = \dfrac{CK_{cs}}{4T_{\mu TC}k_{vs}}$ (here, K_{vs} is the gain coefficient of the voltage sensor).

Figure 3 presents a generator simulation model with a reversible thyristor converter in the charger.

The disadvantage of this scheme is a significant (more than 100%) overadjustment of the charge current at the time of the disturbance appearance with a duration of about 0.6 ms associated with the current pulse passage and the capacitor recharging transient (Fig. 4b). This is due to the large value of the uncompensated time constant of the ACS current loop that is at least 5 ms (see formula (1)), which is 100 times greater than disturbance transit time. Thus, the ACS cannot compensate the disturbance due to inertia, which leads to overadjustment of the charge current at the occurrence time and disturbance development.

To improve the charge current quality, a logic block *BL* blocking the thyristor converter operation and ACS by disabling the control pulses of the thyristor converter, as well as bypassing the PI current regulator *RTZ*, was introduced into the ACS. Figure 4d plots the charge current change after installing the logic device, where overadjustment is completely absent.

Plots of the discharge voltage change on capacitors using non-reversible (Fig. 4e) and reverse (Fig. 4g) converters are shown to compare the transients of voltage (discharge) reduction on the capacitors. When the *BZU* block driving signal is generated to reduce the capacitor voltage, a negative current of 20 A appears on the reversing converter. The voltage processing time, which decreases the reference signal for the reversing converter, is 0.05 ms (Figs. 4f and 4g). In the non-reversible converter, the current's negative component is absent (Fig. 4d) and, therefore, the processing time is 0.12 ms (Figs. 4d and 4e).

The disadvantage of this scheme is the low (less than 200 Hz) pulse repetition rate due to the low-speed ACS performance. This is primarily due to the use of a typical, cheap, but rather inertial thyristor converter based on six connected thyristors according to the Larionov circuit with the uncompensated time constant of 5 ms. To increase the pulse repetition rate up to 400 Hz and higher, it is necessary to use a thyristor converter with a 12-pulse rectification system or a circuit using a frequency converter (for example, based on the "rectifier-filter-inverter" system), which will increase the generator cost.

CONCLUSIONS

The proposed scheme of a current pulse generator with a typical reversible thyristor converter as a charger power supply increases the speed performance of the capacitor's voltage adjustment (amplitude of current pulses). The current diagram's filling factor in capacitor charge (discharge) transients is not lower than 0.7–0.9, which leads to an improvement in the supply network quality. The pulse repetition rate depends on the small time constant of the thyristor converter $T_{\mu TC}$. For the converter based on the Larionov circuit that is considered in this study, $T_{\mu TC} = 5$ ms, and the maximal pulse repetition rate is 200 Hz. The use of higher-quality converters in the charger will increase the pulse repetition rate to 1000 Hz with a slight increase in the generator cost.

FUNDING

This work was supported by the Ministry of Science and Higher Education of the Russian Federation, project no. 3.1283.2017/4.6.

REFERENCES

1. Spitsyn, V.I. and Troitskii, O.A., *Elektroplasticheskaya deformatsiya metalla* (Electroplastic Deformation of Metal), Moscow: Nauka, 1985.
2. Klimov, K.M. and Nevikov, I.I., The "electroplastic effect," *Strength Mater.*, 1984, vol. 16, no. 2, pp. 270–276.
3. Beklemishev, N.N., Working of conducting materials by means of a locally nonuniform pulsed electromagnetic field, *Sov. Electr. Eng.*, 1982, vol. 53, no. 11, pp. 113–117.
4. Klimov, K.M., Shnyrev, G.D., and Novikov, I.I., Change in the ductility of tungsten under the influence of electric current, *Met. Sci. Heat Treat.*, 1977, vol. 19, no. 1, pp. 58–59.
5. Klimov, K.M., Shnyrev, G.D., Novikov, I.I., and Isaev, A.V., Electrostimulated rolling into a tape of micron sections of tungsten and its alloys, *Izv. Akad, Nauk SSSR, Met.*, 1975, no. 4, pp. 143–144.
6. Ye, Y., Kure-Chu, S.-Z., Sun, Z., Li, X., Wang, H., and Tang, G., Nanocrystallization and enhanced surface mechanical properties of commercial pure titanium by electropulsing-assisted ultrasonic surface rolling, *Mater. Des.*, 2018, vol. 149, no. 5, pp. 214–227.
7. Chen, L., Wang, H., Liu, D., Ye, X., Li, X., and Tang, G., Effects of electropulsing cutting on the quenched and tempered 45 steel rods, *J. Wuhan Univ. Technol.- Mater.*, 2018, vol. 33, pp. 204–211.

8. Zhang, R., Li, X., Kuang, J., Li, X., and Tang, G., Texture modification of magnesium alloys during electropulse treatment, *Mater. Sci. Technol.*, 2017, vol. 33, pp. 1421–1427.
9. Li, X., Li, X., Ye, Y., Zhang, R., Kure-Chu, S.-Z., and Tang, G., Deformation mechanisms and recrystallization behavior of Mg–3Al–1Zn and Mg–1Gd alloys deformed by electroplastic-asymmetric rolling, *Mater. Sci. Eng., A*, 2019, vol. 742, pp. 722–733.
10. Ye, Y.-D., Li, X.-P., Sun, Z.-Y., Wang, H.-B., and Tang, G.-Y., Enhanced surface mechanical properties and microstructure evolution of commercial pure titanium under electropulsing-assisted ultrasonic surface rolling process, *Acta Metall. Sin. (Engl. Lett.)*, 2018, vol. 31, no. 12, pp. 1272–1280.
11. Tang, G., Zhang, J., Yan, Y., Zhou, H., and Fang, W., The engineering application of the electroplastic effect in the cold-drawing of stainless steel wire, *J. Mater. Process. Technol.*, 2003, vol. 137, no. 1, pp. 96–99.
12. Kozlov, A., Mordyuk, B., and Chemyashevsky, A., On the additivity of acoustoplastic and electroplastic effects, *Mater. Sci. Eng., A*, 1995, vol. 190, no. 1, pp. 75–79.
13. Ruszkiewicz, B.J., Grimm, T., Ragai, I., Mears, L., and Roth, J.T., A review of electrically-assisted manufacturing with emphasis on modeling and understanding of the electroplastic effect, *J. Manuf. Sci. Eng.*, 2017, vol. 139, no. 11, pp. 110801-1–110801-15.
14. Fan, G., Sun, F., Meng, X., Gao, L., and Tong, G., Electric hot incremental forming of Ti–6A1–4V titanium sheet, *Int. J. Adv. Manuf. Technol.*, 2010, vol. 49, nos. 9–12, pp. 941–947.
15. Fan, G., Gao, L., Hussain, G., and Wu, Z., Electric hot incremental forming: a novel technique, *Int. J. Mach. Tools Manuf.*, 2008, vol. 48, no. 15, pp. 1688–1692.
16. Shi, X., Gao, L., Khalatbari, H., Xu, Y., Wang, H., and Jin, L., Electric hot incremental forming of low carbon steel sheet: accuracy improvement, *Int. J. Adv. Manuf. Technol.*, 2013, vol. 68, nos. 1–4, pp. 241–247.
17. Bao, W., Chu, X., Lin, S., and Gao, J., Experimental investigation on formability and microstructure of AZ31B alloy in electropulse-assisted incremental forming, *Mater. Des.*, 2015, vol. 87, pp. 632–639.
18. Honarpisheh, M., Abdolhoseini, M., and Amini, S., Experimental and numerical investigation of the hot incremental forming of Ti–6A1–4V sheet using electrical current, *Int. J. Adv. Manuf. Technol.*, 2016, vol. 83, nos. 9–12, pp. 2027–2037.
19. Xu, D., Lu, B., Cao, T., Zhang, H., Chen, J., Long, H., and Cao, J., Enhancement of process capabilities in electrically-assisted double sided incremental forming, *Mater. Des.*, 2016, vol. 92, pp. 268–280.
20. Liu, R., Lu, B., Xu, D., Chen, J., Chen, F., Ou, H., and Long, H., Development of novel tools for electricity-assisted incremental sheet forming of titanium alloy, *Int. J. Adv. Manuf. Technol.*, 2016, vol. 85, nos. 5–8, pp. 1137–1144.
21. Xie, H., Dong, X., Peng, F., Wang, Q., Liu, K., Wang, X., and Chen, F., Investigation on the electrically-assisted stress relaxation of AZ31B magnesium alloy sheet, *J. Mater. Process. Technol.*, 2016, vol. 227, pp. 88–95.
22. Adams, D. and Jeswiet, J., Single-point incremental forming of 6061-T6 using electrically assisted forming methods, *Proc. Inst. Mech. Eng.*, 2014, vol. 228, no. 7, pp. 757–764.
23. Valoppi, B., Egea, A.J.S., Zhang, Z., Rojas, H.A.G., Ghiotti, A., Bruschi, S., and Cao, J., A hybrid mixed double-sided incremental forming method for forming Ti6A14V alloy, *CIRP Ann.*, 2016, vol. 65, no. 1, pp. 309–312.
24. Nguyen-Tran, H., Oh, H., Hong, S., Han, H.N., Cao, J., Ahn, S., and Chun, D., A review of electrically-assisted manufacturing, *Int. J. Precis.: Eng. Manuf. Green Technol.*, 2015, vol. 2, no. 4, pp. 365–376.
25. Guan, L., Tang, G., and Chu, P.K., Recent advances and challenges in electroplastic manufacturing processing of metals, *J. Mater. Res.*, 2010, vol. 25, no. 7, pp. 1215–1224.
26. Kuznetsov, V.A., Gromov, V.E., and Simakov, V.P., USSR Inventor's Certificate no. 884092, *Byull. Izobret.*, 1981, no. 43.
27. Kuznetsov, V.A. and Gromov, V.E., Effective high power pulse generator, *Izv. Vyssh. Uchebn. Zaved., Elektromekh.*, 1986, no. 6, pp. 122–124.
28. Zhmakin, Yu.D., Zagulyaev, D.V., Konovalov, S.V., Kuznetsov, V.A., and Gromov, V.E., High power current pulse generator for intensification of metal forming, *Izv. Vyssh. Uchebn. Zaved., Chern. Metall.*, 2008, no. 8, pp. 42–44.
29. Kuznetsov, V.A., Polkovnikov, G.D., Kuznetsova, E.S., and Gromov, V.E., Development of automatic control system for electrostimulated drawing using high power current pulses, *Trudy Vos'moi Vserossiiskoi nauchno-prakticheskoi konferentsii "Avtomatizirovannyi elektroprivod i promyshlennaya elektronika"* (Proc Eight All-Russ. Sci.-Pract. Conf. "Automated Electric Drive and Industrial Electronics"), Ostrovlyanchik, V.Yu., Ed., Novokuznetsk: Sib. Gos. Ind. Univ., 2018, pp. 132–138.
30. Onishchenko, G.B., Aksenov, M.I., and Grekhov, V.P., *Avtomatizirovannyi elektroprivod promyshlennykh ustanovok (Automated Electric Drive of Industrial Units)*, Onishchenko, G.B., Ed., Moscow: Ross. Akad. S-kh. Nauk, 2001.

Translated by A. Ivanov